



## NMR experiments for the measurement of proton–proton and carbon–carbon residual dipolar couplings in uniformly labelled oligosaccharides

Manuel Martín-Pastor<sup>a,\*</sup>, Angeles Canales-Mayordomo<sup>b</sup> and Jesús Jiménez-Barbero<sup>b,\*</sup>

<sup>a</sup>Laboratorio Integral de Estructura de Biomoléculas Jose. R. Carracido, Unidad de Resonancia Magnética, RIAIDT, Universidad de Santiago de Compostela, 15782 Santiago de Compostela, Spain; <sup>a</sup>Departamento de Estructura y función de proteínas, Centro de Investigaciones Biológicas, CSIC, Ramiro de Maeztu 9, 28040 Madrid, Spain

Received 28 January 2003; Accepted 11 April 2003

**Key words:** carbon–carbon couplings, NMR, oligosaccharide conformation, residual dipolar couplings

### Abstract

A 2D-HSQC-carbon selective/proton selective-constant time COSY, 2D-HSQC-(sel C, sel H)-CT COSY experiment, which is applicable to uniformly <sup>13</sup>C isotopically enriched samples (U-<sup>13</sup>C) of oligosaccharides or oligonucleotides is proposed for the measurement of proton–proton RDC in crowded regions of 2D-spectra. In addition, a heteronuclear constant time-COSY experiment, <sup>13</sup>C-<sup>13</sup>C CT-COSY, is proposed for the measurement of one bond carbon–carbon RDC in these molecules. These two methods provide an extension, to U-<sup>13</sup>C molecules, of the original homonuclear constant time-COSY experiment proposed by Tian et al. (1999) for saccharides. The combination of a number of these RDC with NOE data may provide the method of choice to study oligosaccharide conformation in the free and receptor-bound state.

**Abbreviations:** RDC – Residual Dipolar coupling; CT-COSY – constant time COSY; CT-HSQC – constant time HSQC; HSQC (sel C, sel H)-CT COSY HSQC – selectively edited in <sup>13</sup>C and <sup>1</sup>H, constant time COSY; U-<sup>13</sup>C – uniformly <sup>13</sup>C isotopically enriched sample.

### Introduction

Carbohydrates serve as recognition molecules in numerous biological processes (Dwek, 1996; Gabius and Gabius, 1997). Knowledge of the three-dimensional structure and dynamic properties of the carbohydrate moieties both free in solution and in the bound state with their receptors, are essential for understanding the biological events in which glycoconjugates are involved.

NMR is currently the method of choice to deduce carbohydrate conformation and dynamics (Jiménez-Barbero and Peters, 2002). Due to the frequent lack of enough number of NOEs to unambiguously de-

duce the conformational properties of oligosaccharides, residual dipolar couplings (RDC) (Tjandra et al., 1997; Prestegard, 1998) have emerged as a key complement of NOEs to perform NMR-based structural studies of these biomolecules (Lycknert et al., 2001; Martín-Pastor and Bush, 2001; Neubauer et al., 2001).

Carbohydrate spectra are often very crowded, making difficult the complete analysis of the NMR parameters. However, the use of <sup>13</sup>C labeled material may alleviate this problem, as shown below. In fact, in contrast to protein or nucleic acid NMR, the development of carbohydrate NMR has been hampered by the difficulty of obtaining <sup>13</sup>C labeled material by chemical or chemoenzymatic synthesis. However, provided that <sup>13</sup>C labeled oligosaccharides are available, a new repertory of NMR experiments may permit the ac-

\*To whom correspondence should be addressed. E-mails: jjbarbero@cib.csic.es; mmartin@usc.es

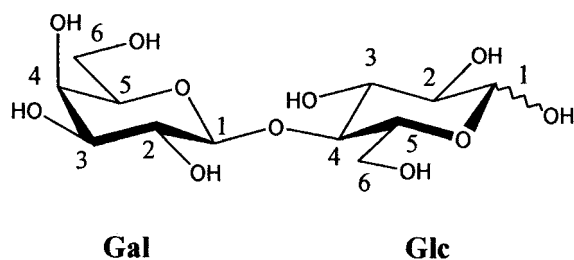


Figure 1. Schematic view of lactose (**1**) showing the atomic numbering. Both GLC- $\alpha$  and GLC- $\beta$  anomers are present in solution.

cess to additional key parameters as RDC (Tjandra and Bax, 1997). Indeed, RDC are frequently used for the refinement of 3D structures of proteins, and the availability of  $^{15}\text{N}$ -labeled polypeptides makes their measurement and application a relatively accessible task. Thus, the combined use of NOEs, scalar couplings, RDC and/or cross-correlated relaxation rates techniques may be envisaged as the method of choice to analyze carbohydrate conformation in a rigorous manner (Bose et al., 1998; Cloran et al., 2000; Vincent and Zwahlen, 2000; Martin-Pastor and Bush, 2001; Freedberg, 2002).

From the RDC perspective, a CT-COSY experiment (Tian et al., 1999, 2001) has been proposed for the quantitative measurement of proton-proton scalar and RDC couplings  $^nJ_{\text{HH}}$  ( $+^nD_{\text{HH}}$ ) which has been applied to biomolecules at natural abundance. In the original method, signal overlapping poses a problem to quantify the couplings, although an alternative analysis has also been proposed (Wu and Bax, 2001). A 3D  $^{15}\text{N}$  edited version of the CT-COSY experiment has also been described (Tian et al., 2000).

On this basis, and to generalize the measurement of homonuclear RDCs, we herein report on two new methods for the determination of  $D_{\text{HH}}$  and  $D_{\text{CC}}$  in  $^{13}\text{C}$  uniformly enriched oligosaccharides, which may be combined with  $^1\text{D}_{\text{CH}}$  to obtain the carbohydrate conformation in a NOE-independent manner.

## Experimental section

### Sample preparation

The synthesis of uniformly  $^{13}\text{C}$  labelled ( $\text{U-}^{13}\text{C}$ ) lactose (Figure 1) will be described elsewhere, although was based on the method of Field and coworkers. (Shimizu et al., 1998). A sample was prepared by dissolving 5 mg of  $\text{U-}^{13}\text{C}$  lactose in  $\text{D}_2\text{O}$ . For the measurement of RDC, an alignment medium consist-

ing in cetylpyridinium chloride (CPCI)/hexanol 1:1 and brine (0.2 M NaCl) (Porte et al., 1986; Gomati et al., 1987; Prosser et al., 1998) was used. This system forms a positively charged lamellar phase, which has previously been used to orient carbohydrates (Rundlöf et al., 1998; Martin-Pastor and Bush, 2001). Two oriented samples of **1** were prepared by dissolving 5 mg of  $\text{U-}^{13}\text{C}$  lactose in the medium at a CPCI/hexanol/brine concentration of 5% and 10% (w/w), respectively. These two samples are referred in the text as CPCI 5% and CPCI 10%, respectively. The presence of alignment was monitored by observing a symmetric quadrupolar splitting on the deuterium  $\text{D}_2\text{O}$  lock signal, proportional to the degree of alignment achieved. In the present case, the splittings were 16.2 Hz (5%) and 44.7 Hz (10%).

### NMR spectroscopy

Experiments were acquired at 25 °C on a Varian INOVA NMR instrument operating at 750 MHz and processed with MestRe-C v3.0 software (Cobas and Sardina, 2003). Origin v6.1 (OriginLab Corporation, <http://www.OriginLab.com>) was used to fit the integrals according to Methods I or II (see below) providing the corresponding scalar (or scalar + RDC) couplings. RDC were determined by subtraction of the values for the oriented and non-oriented sample (Tjandra and Bax, 1997).

A constant time HSQC experiment (Santoro and King, 1992; Vuister and Bax, 1992) was acquired for a sample of **1** in  $\text{D}_2\text{O}$  (Figure S1 in the supplementary material). This experiment was instrumental to choose the regions for measuring the RDC.

### Measurement of proton-proton $^nJ_{\text{HH}}$ ( $+^nD_{\text{HH}}$ ) couplings

These measurements were performed for **1** in  $\text{D}_2\text{O}$  and in the CPCI 5% oriented medium, using the 2D HSQC (sel C, sel H) CT-COSY sequence of Figure 2. Selective (or semiselective)  $^1\text{H}$  and  $^{13}\text{C}$  pulses were properly calibrated and adjusted to measure certain  $^nJ_{\text{HH}}$  ( $+^nD_{\text{HH}}$ ) located in a chosen region in the CT-HSQC spectrum (Figure S1). Five proton-carbon regions were considered: a) Gal 1 + Glc $\beta$  1 + Glc $\alpha$  1, b) Gal 3, c) Glc $\beta$  2 + Gal 2, d) Glc $\alpha$  $\beta$  4, and e) Gal 4 + Glc $\alpha$  5. In all cases, the  $^1\text{H}$  spectral window covered all the proton resonances. For the  $^{13}\text{C}$  dimension, reduced spectral windows were used. For region (a) the carbon carrier was set at 95 ppm, the  $^{13}\text{C}$  spectral width was 28 ppm, the delay  $\tau$  was set to 1.47 ms and a

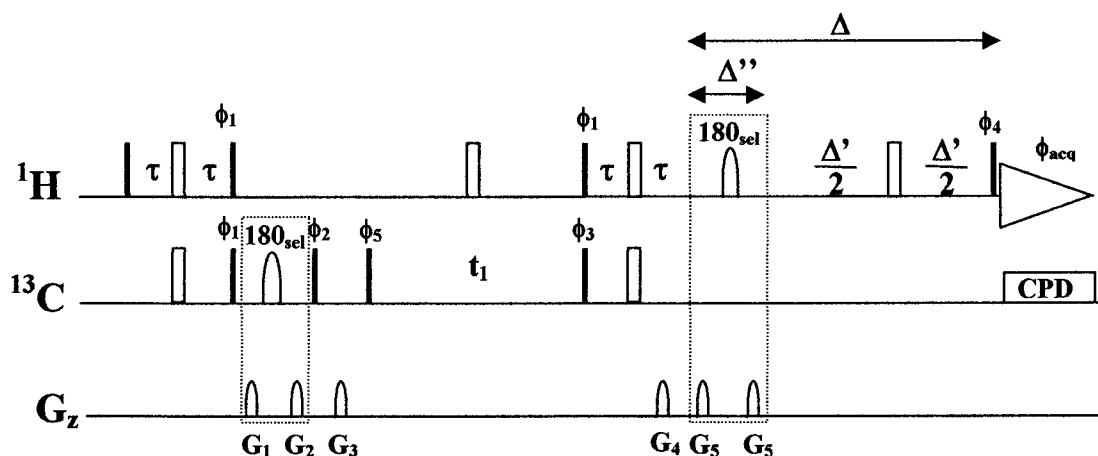


Figure 2. Pulse sequence for the 2D HSQC (selC, sel H) CT-COSY experiment. Pulses of  $90^\circ$  and  $180^\circ$  are represented by filled and open bars, respectively, with the phase  $x$  unless indicated. Phase cycling was as follows:  $\phi_1 = y$ ,  $\phi_2 = -y$ ,  $\phi_3 = x$ ,  $-x$ ,  $\phi_4 = x$ ,  $x$ ,  $y$ ,  $y$ ,  $-x$ ,  $-x$ ,  $-y$ ,  $-y$ ,  $\phi_{\text{acq}} = x$ ,  $-x$ ,  $-x$ ,  $x$ . Quadrature detection in  $t_1$  was obtained alternating  $\phi_5$  with the States method. Gradients are square shaped with duration of 1 ms and amplitudes  $G_{1,2,3,4,5} = 10, 42, 12, 8, 10$  G/cm. Delay duration  $\tau$  corresponds to  $(4J_{\text{CH}})^{-1}$  and the  $180^\circ$  shaped pulses were of the refocusing Snob type (Kupce et al., 1995).

semi-selective  $^{13}\text{C}$  pulse of 0.693 ms was used. In this case, the  $180^\circ$   $^1\text{H}$  pulse was a non-selective squared hard pulse. For regions (b) to (e) the  $^{13}\text{C}$  carrier was set to 74 ppm, the  $^{13}\text{C}$  spectral width was 16 ppm, and the delay  $\tau$  was set to 1.72 ms. The semi-selective  $180^\circ$   $^{13}\text{C}/^1\text{H}$  pulse widths were 8.83/9.37 ms, 1.18/9.76 ms, 2.33/7.93, and 4.41/12.01 ms for regions b, c, d, and e, respectively. Refocusing snob-type pulses were employed (Kupce et al., 1995), calibrated with the Pandora's Box routine provided with the spectrometer software.

For a given sample, and for each region selected, fourteen 2D HSQC (sel C, sel H) CT-COSY experiments were acquired under the same conditions, except for the CT-delays  $\Delta$ , which were varied from 0.08 to 0.24 s. 8 scans and 64  $t_1$  increments were used, resulting in a total acquisition time of  $\sim 18$  min for each spectrum. The extraction of the  $^nJ_{\text{HH}}$  ( $+^nD_{\text{HH}}$ ) was done according to Method I (see theory section). As a reference of the sensitivity achieved with this sequence, the signal to noise ratio of the direct Gal H1/C1 peak was 62 with the  $\text{D}_2\text{O}$  sample and a  $\Delta$  value of 80 ms.

2D  $^1\text{H}$ - $^1\text{H}$  CT-COSY experiments (Tian et al., 1999) were acquired for the determination of  $^nJ_{\text{HH}}$  ( $+^nD_{\text{HH}}$ ) in the  $\text{D}_2\text{O}$  and CPCI 5% samples of **1**. A Broad-band  $^{13}\text{C}$  garp decoupling scheme was applied during both constant time and acquisition periods to remove the proton-carbon couplings. An acquisition time of 100 ms was used. A total of  $330 \times 128$  com-

plex points were acquired for the  $t_2$  and  $t_1$  dimensions with 8 scans per  $t_1$  increment. Fourteen experiments were with CT-delays  $\Delta$  varying from 0.08 to 0.225 s, resulting in total acquisition times of  $\sim 1$  h for each experiment. The extraction of the  $^nJ_{\text{HH}}$  ( $+^nD_{\text{HH}}$ ) of **1** was done according to Method I.

#### Measurement of one bond carbon-carbon couplings $^1J_{\text{CC}}$ ( $+^1D_{\text{CC}}$ ) and long range $^nJ_{\text{CC}}$ couplings

These couplings were determined using a series of  $^{13}\text{C}$ - $^{13}\text{C}$  CT-COSY experiments (Tian et al., 1999; Wu and Bax, 2001). The decoupler was set to the proton channel and a WALTZ-16 low power scheme was applied during the complete sequence. Fourteen experiments were acquired with CT-delays  $\Delta$  varying from 0.015 to 0.050 s. The  $^{13}\text{C}$  carrier was set at 80 ppm with a spectral width of 60 ppm, covering all the  $^{13}\text{C}$  resonances of **1**. A total of 1024 complex points were acquired with 128  $t_1$  increments and 8 scans per increment ( $\sim 1$  h). The extraction of  $^1J_{\text{CC}}$  ( $+^1D_{\text{CC}}$ ) was performed using method I.  $^1D_{\text{CC}}$  values were obtained by subtracting the results obtained with the CPCI 5% or 10% oriented samples from the  $\text{D}_2\text{O}$  one.

For long range  $^nJ_{\text{CC}}$ , an additional set of fourteen experiments were acquired with CT-delays  $\Delta$  varying from 50 to 150 ms. The extraction of  $^nJ_{\text{CC}}$  was performed using Method II.

## Theory

### Extraction of the $J + \text{RDC}$ couplings

#### Method I (active coupling determination).

Following the scheme proposed by Tian et al. (1999, 2000, 2001), both the cross peaks,  $I_{\text{cross}}$ , and the corresponding diagonal peaks,  $I_{\text{auto}}$ , were integrated. The  $I_{\text{cross}}/I_{\text{auto}}$  ratio obtained at each  $\Delta$  was fitted to Equation 1.

$$J + D = k \arctan(I_{\text{cross}}/I_{\text{auto}})/\pi\Delta, \quad (1)$$

where  $J$  and  $D$  represent the scalar and the RDC couplings,  $k$  is a scaling factor, and  $\Delta$  is the constant time.

#### Method II (passive coupling determination).

The original cross peak nulling method proposed by Wu and Bax (2001) was modified for the determination of the  ${}^n\text{J}_{\text{CC}}$  with the  ${}^{13}\text{C}$ - ${}^{13}\text{C}$  CT-COSY experiment.

The cross-peak intensity corresponding to the  ${}^1\text{J}_{\text{CC}}$  active coupling (1-bond), is proportional to a combination of the active and passive couplings involved according to Equation 2.

$$\begin{aligned} I_{\text{cross}}^{1\text{-bond}} &\propto \sin(\pi * {}^1\text{J}_{\text{CCactive}} * \Delta) * \\ &\Pi \cos(\pi * {}^1\text{J}_{\text{CCpassive}} * \Delta) * \\ &\Pi \cos(\pi * {}^n\text{J}_{\text{CCpassive}} * \Delta). \end{aligned} \quad (2)$$

Analogously, the intensity of a cross-peak corresponding to a long range active coupling ( $n$ -bond) is given by Equation 3.

$$\begin{aligned} I_{\text{cross}}^{n\text{-bond}} &\propto \sin(\pi * {}^n\text{J}_{\text{CCactive}} * \Delta) * \\ &\Pi \cos(\pi * {}^1\text{J}_{\text{CCpassive}} * \Delta) * \\ &\Pi \cos(\pi * {}^n\text{J}_{\text{CCpassive}} * \Delta). \end{aligned} \quad (3)$$

For a pair of  $I_{\text{cross}}^{1\text{-bond}}$  and  $I_{\text{cross}}^{n\text{-bond}}$  sharing the same diagonal peak, it is possible to define the ratio of its intensities,  $I'_{\text{cross}}$ , according to Equation 4.

$$\begin{aligned} I'_{\text{cross}} = I_{\text{cross}}^{1\text{-bond}}/I_{\text{cross}}^{n\text{-bond}} &\propto \tan \\ &(\pi * {}^1\text{J}_{\text{CC}} * \Delta) * \text{cotag}(\pi * {}^n\text{J}_{\text{CC}} * \Delta). \end{aligned} \quad (4)$$

$I'_{\text{cross}}$  only depends on the  ${}^1\text{J}_{\text{CC}}$  and  ${}^n\text{J}_{\text{CC}}$  couplings. Other possible passive couplings affecting the cross peaks are cancelled out. The constant time  $\Delta_{\text{null}}$  for which  $I'_{\text{cross}} = 0$  allows to extract either  ${}^n\text{J}_{\text{CC}}$  or  ${}^1\text{J}_{\text{CC}}$  couplings. The following  $I'_{\text{cross}}$  nulling conditions can be deduced:

$${}^1\text{J}_{\text{CC}} = n/\Delta_{\text{null}} \quad \text{for } n = 1, 2, 3, \dots, \quad (5a)$$

$${}^n\text{J}_{\text{CC}} = 1/(2\Delta_{\text{null}}). \quad (5b)$$

Given the large difference in magnitude between  ${}^1\text{J}_{\text{CC}}$  and  ${}^n\text{J}_{\text{CC}}$ , it is possible to extract  ${}^1\text{J}_{\text{CC}}$  directly from the first null in  $I'_{\text{cross}}$  obtained at short constant times ( $\Delta < 70$  ms), using Equation 5a. For longer  $\Delta$  values (100–200 ms) the nulls in  $I'_{\text{cross}}$  corresponds to either  ${}^1\text{J}_{\text{CC}}$  or  ${}^n\text{J}_{\text{CC}}$ . Once  ${}^1\text{J}_{\text{CC}}$  has been determined, Equation 5a allows to distinguish those  $\Delta_{\text{null}}$  corresponding to  ${}^1\text{J}_{\text{CC}}$ , while the remainder  $\Delta_{\text{null}}$ , corresponding to  ${}^n\text{J}_{\text{CC}}$ , can be determined using Equation 5b.

## Results and discussion

### Measurement of ${}^n\text{J}_{\text{HH}}$ and ${}^n\text{D}_{\text{HH}}$

The methodology described herein permits to determine a set of homonuclear RDCs (both  ${}^1\text{H}$ - ${}^1\text{H}$  and  ${}^{13}\text{C}$ - ${}^{13}\text{C}$ ) that may allow to deduce carbohydrate (or nucleic acid) conformation in solution (Freedberg, 2002). A 2D CT-COSY has been described (Tian et al., 1999, 2000, 2001) which allows to determine  ${}^n\text{J}_{\text{HH}}$  and  ${}^n\text{D}_{\text{HH}}$ . Nevertheless, the typical proton signal overlapping in saccharides prevent the measurement of many couplings in this way. Herein, the access to  $\text{U-}{}^{13}\text{C}$  samples offers the possibility to alleviate this difficulty by using the  ${}^{13}\text{C}$  dimension. Instead of increasing the dimensionality of the experiment to 3D, which is very time consuming because the method requires acquiring several experiments with different CT-delays, we have chosen a method which employs semi-selective proton and carbon pulses, within a 2D  ${}^1\text{H}/{}^{13}\text{C}$  correlation experiment. The proposed sequence (Figure 2) is a 2D-HSQC-selective carbon/selective proton- CT-COSY, dubbed 2D HSQC(sel C, sel H) CT-COSY.

The sequence starts by converting the initial  ${}^1\text{H}$  magnetization to antiphase  ${}^1\text{H}$ - ${}^{13}\text{C}$  magnetization with the first INEPT block. This is followed by a  $180^\circ$  semi-selective  ${}^{13}\text{C}$  pulse inserted as a gradient spin echo, which allows to select the desired auto-peak/s. Those auto-peaks not refocused by the pulse will be defocused by the effect of the  $G_1$  and  $G_2$  gradients and will not be observed. The sequence proceeds with a  $z$ -filter, which retains only one component of the antiphase magnetization created prior to the  $t_1$  carbon chemical shift evolution period. After this  $t_1$  period, the subsequent reverse INEPT transfers magnetization back to  ${}^1\text{H}$ . At this point, a  $180^\circ$  semiselective  ${}^1\text{H}$  pulse

inserted in the middle of a gradient spin echo serves to further select the desired auto-peak/s according to their  $^1\text{H}$  chemical shift. This step is then followed by a CT-COSY period to transfer magnetization from the selected auto-peak/s to the coupled protons, which will be detected during  $t_2$ . In the scheme of Figure 2, the homonuclear couplings evolve during a total constant time period  $\Delta = \Delta' + \Delta''$ , which include the time corresponding to the semi-selective proton gradient echo. Gradients  $G_2$ ,  $G_3$  and  $G_4$  are used to encode the carbon coherences  $1 \cdot \gamma_{\text{C}}$ ,  $0$ ,  $-1 \cdot \gamma_{\text{H}}$ , respectively, which must fulfill the condition  $G_2 = 4 G_4 + G_1$ .

The experiment was applied to U- $^{13}\text{C}$  lactose (**1**, Figure 1). The assignment of the NMR signals of **1** (Bock et al., 1984; Platzer et al., 1989) was confirmed with standard methods. A CT-HSQC permitted to decide on the selectivity required for the shaped  $^{13}\text{C}$  and  $^1\text{H}$  pulses. The five regions in the CT-HSQC described in the experimental part were considered (Figure S1 in the supplementary material, available from the authors) for the measurement of  $^n\text{J}_{\text{HH}}(+^n\text{D}_{\text{HH}})$ .

The HSQC (sel C, sel H) CT-COSY spectra of **1** showed the expected COSY cross peaks for each selected auto-peak. Inspection of the spectra of the oriented sample revealed the presence of additional cross peaks, which are only mediated by RDC. One key example is Gal 1-Glc $\beta$  4 (Figure 3). Indeed, this interaction is not completely unexpected, since it corresponds to a NOE experimentally observed in isotropic solution, that defines the major orientation around  $\Phi/\Psi$  torsion angles in solution (Asensio et al., 1995). However, the RDC provides angular orientation with respect to the magnetic field, it is not contaminated by spin diffusion and its sensitivity to the inter-nuclear internal motions  $\langle r^{-3} \rangle$  is in a different time scale to that of NOEs (Tian et al., 2000). In this regard, the combined information provided by RDC and NOE could be useful to study the potential flexibility among the two sugar units that define the glycosidic angles.

The peak integrals of the HSQC (sel C, sel H) CT-COSY were fitted to obtain  $^n\text{J}_{\text{HH}}(+^n\text{D}_{\text{HH}})$  by using Method I. The results are given in Figure 4a and in Table 1. Some additional examples of fitting are given in Figure S2 in the supplementary material. For those peaks only mediated by RDC (i.e., Gal 1-3 and Gal 1-Glc $\beta$  4), this quantitative experiment only provides the magnitude, but not the sign of  $^n\text{D}_{\text{HH}}$  (Tian et al., 1999, 2000, 2001). Nevertheless, the method reported herein may be complemented by that recently described for sign discrimination (Peti and Griesinger, 2000).

The  $^n\text{J}_{\text{HH}}(+^n\text{D}_{\text{HH}})$  values obtained with the method of Figure 2 were very similar to those that could also be obtained with the original  $^1\text{H}$ - $^1\text{H}$  CT-COSY sequence (Tian et al., 1999) as shown in Figure 3b and Table 1. However, the scheme of Figure 2 permitted to determine and to quantify additional couplings. The relative sensitivity between these two experiments was experimentally determined on the basis of the signal to noise ratio for spectra acquired and processed under identical conditions (same sample, number of scans,  $\Delta$ , etc). The sequence of Fig. 2 was ca. half less sensitive than the CT-COSY.

#### Measurement of $^1\text{J}_{\text{CC}}$ and $^1\text{D}_{\text{CC}}$

$^1\text{D}_{\text{CC}}$  also possess key conformational information for oligosaccharides. In fact, for each monosaccharide in a regular chair conformation, a total of five  $^1\text{D}_{\text{CC}}$  vectors, four of them with independent orientations, could possibly be determined and used to determine the pyranose chair and/or global saccharide conformation. In principle,  $^1\text{J}_{\text{CC}}(+^1\text{D}_{\text{CC}})$  could be measured from the splittings in regular 1D  $^{13}\text{C}$  NMR experiments using broadband  $^1\text{H}$ -decoupling for small sugars (Freedberg, 2002). However, the usual  $^{13}\text{C}$  linewidths for longer saccharides in these spectra ( $\sim 11.5$  Hz for **1**, just a disaccharide, in  $\text{D}_2\text{O}$ ) reduces considerably their accuracy. Apart of the potential ambiguous assignment with 1D experiments, accurate  $^1\text{D}_{\text{CC}}$  values are crucial, given the rather small magnitude of the obtained values ( $< 4$  Hz) at the used concentrations of the orienting media. Thus, we determined the  $^1\text{J}_{\text{CC}}(+^1\text{D}_{\text{CC}})$  values by using a 2D  $^{13}\text{C}$ - $^{13}\text{C}$  CT-COSY experiment under broadband  $^1\text{H}$ -decoupling, a variation of the CT-COSY experiment (Tian et al., 1999, 2000, 2001; Wu and Bax, 2001). This sequence is simpler than other inversion-detected schemes, also proposed to measure  $\text{J}_{\text{CC}}$  in U- $^{13}\text{C}$  samples (Bax et al., 1992; Hu and Bax, 1996, 1997). In addition, since protons are decoupled during the complete experiment, there is no need to handle the  $^1\text{H}$ - $^{13}\text{C}$  couplings, thus reducing their possible effects on quantitation (Bax et al., 1992).

The intensities of the 2D  $^{13}\text{C}$ - $^{13}\text{C}$  CT-COSY experiments (Figure 5) were fitted with Method I to obtain the results of Table 2. Some examples of fitting curves are given in Figures S3 and S4 in the supplementary material. The  $^1\text{D}_{\text{CC}}$  values are small, with the exception of Gal C3-C4 and Gal C5-C6, and the method offers good accuracy with fitting errors in the range 0.05–0.15 Hz.

Table 1.  ${}^nJ_{\text{HH}}$  ( $+{}^nD_{\text{HH}}$ ) of **1** obtained at 25 °C for the  $\text{D}_2\text{O}$  non-oriented and CPCI 5% oriented samples with 2D HSQC (selC, selH) CT-COSY<sup>a</sup> and  ${}^1\text{H}$ - ${}^1\text{H}$  CT-COSY<sup>b</sup> (Tian et al., 1999). Reference values are taken from Bock et al. (1984) and Platzer et al. (1989)

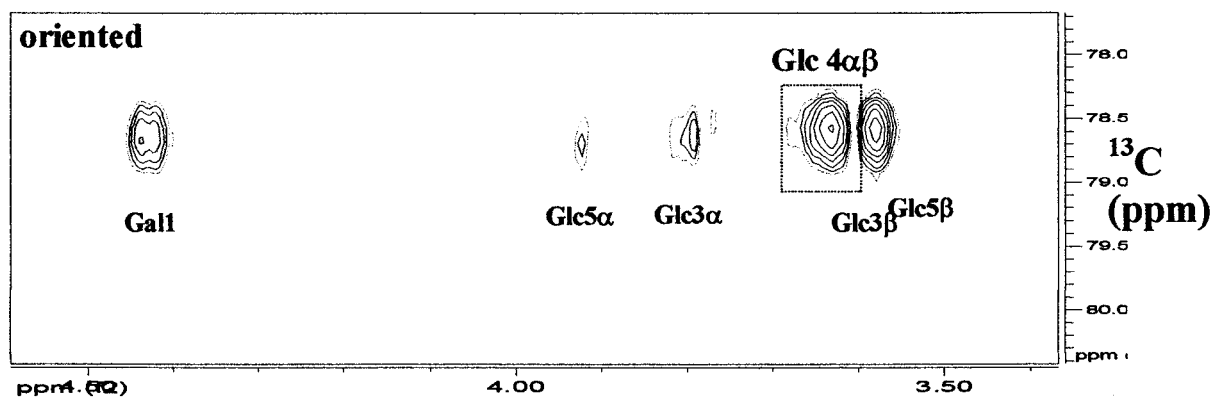
	Ref.	${}^nJ_{\text{HH}}$ (Hz) <sup>a</sup>	${}^nJ_{\text{HH}}+{}^nD_{\text{HH}}$ (Hz) <sup>a</sup>	${}^nD_{\text{HH}}$ (Hz) <sup>a</sup>	${}^nJ_{\text{HH}}$ (Hz) <sup>b</sup>	${}^nJ_{\text{HH}}+{}^nD_{\text{HH}}$ (Hz) <sup>b</sup>	${}^nD_{\text{HH}}$ (Hz) <sup>b</sup>
Gal 1-2	7.8	7.9	8.5	0.6	7.8	8.5	0.7
Gal 1-3	0.0	0.0	$\pm 3.8$	$\pm 2.8^\ddagger$	ovlp.	ovlp.	ovlp.
Gal 2-3	10.0	10.1	10.4	0.3	10.0	10.3	0.3
Gal 3-4	3.4	3.0	3.3	0.3	ovlp.	ovlp.	ovlp.
Gal Glc $\beta$ 4	0.0	0.0	4.4	$\pm 4.4^\ddagger$	ovlp.	ovlp.	ovlp.
Glc $\beta$ 1-2	7.9	8.1	0.1	7.8	7.8	8.0	0.2
Glc $\beta$ 2-3	8.9	8.7	8.4	-0.3	8.7	8.4	-0.3
Glc $\alpha$ 1-2	3.7	3.7	*		3.6	*	

\*Bad fit.

<sup>‡</sup>Sign cannot be determined.

ovlp. Overlap precludes proper integration.

a)



b)

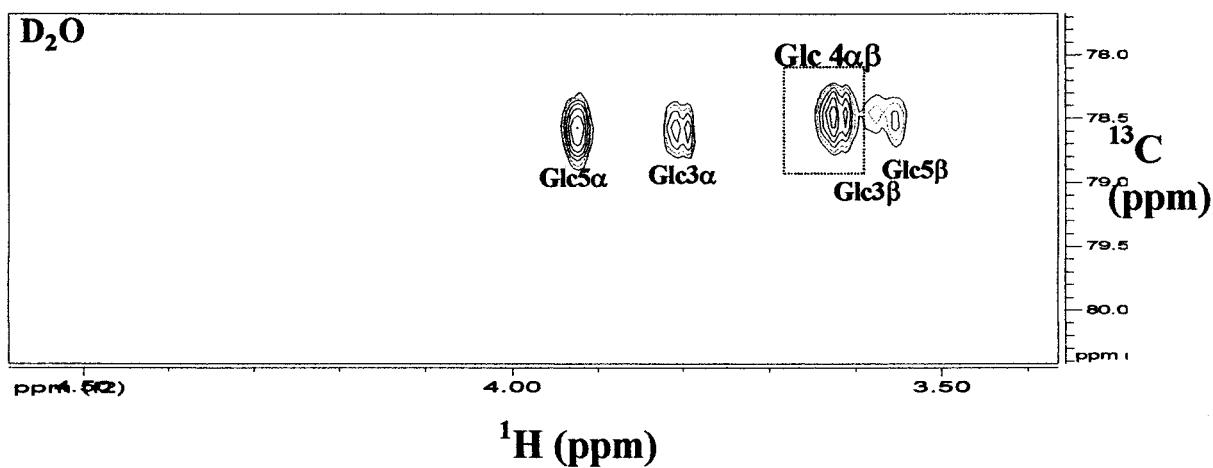


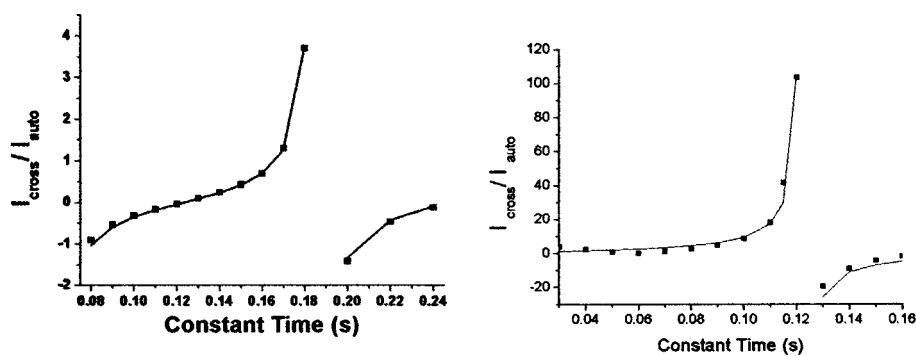
Figure 3. 2D HSQC (sel C, sel H) CT-COSY spectra of **1** with selection of the Glc 4 ( $\alpha + \beta$ ) signal. (a) CPCI 5%, oriented sample (b)  $\text{D}_2\text{O}$ , Non-oriented sample.

Table 2.  $^1J_{CC}$  ( $+^1D_{CC}$ ) obtained for **1** at 25 ° C for the D<sub>2</sub>O non-oriented and the oriented samples (CPCI 5%) and (CPCI 10%)

	D <sub>2</sub> O $^1J_{CC}$ (Hz)	CPCI 5% $^1J_{CC}+^1D_{CC}$ (Hz)	CPCI 5% $^1D_{CC}$ (Hz)	CPCI 10% $^1J_{CC}+^1D_{CC}$ (Hz)	CPCI 10% $^1D_{CC}$ (Hz)
Gal 1-2	48.76 ± 0.10	48.62 ± 0.10	-0.1	48.00 ± 0.10	-0.6
Gal 2-3	39.16 ± 0.05	38.92 ± 0.10	-0.2	38.40 ± 0.10	-0.8
Gal 3-4	40.48 ± 0.15	41.64 ± 0.15	1.2	41.59 ± 0.10	1.1
Gal 4-5	39.28 ± 0.05	39.02 ± 0.05	-0.3	38.37 ± 0.10	-0.9
Gal 5-6	44.42 ± 0.15	47.33 ± 0.10	2.9	48.22 ± 0.10	3.8
Glcβ 1-2	48.02 ± 0.10	48.14 ± 0.10	0.1	48.08 ± 0.10	0.1
Glcβ 5-6	44.19 ± 0.10	44.53 ± 0.10	0.3	45.48 ± 0.05	1.3
Glcα 1-2	44.84 ± 0.15	44.62 ± 0.15	-0.2	44.60 ± 0.15	-0.2
Glcα 4-5 <sup>a</sup>	40.88 ± 0.10	41.17 ± 0.10	0.3	41.11 ± 0.10	0.2
Glcα 5-6	44.21 ± 0.15	44.12 ± 0.15	-0.1	45.51 ± 0.15	1.3

<sup>a</sup>Auto peak corresponds to Glcα 4 + Glcβ 4.

a)



b)

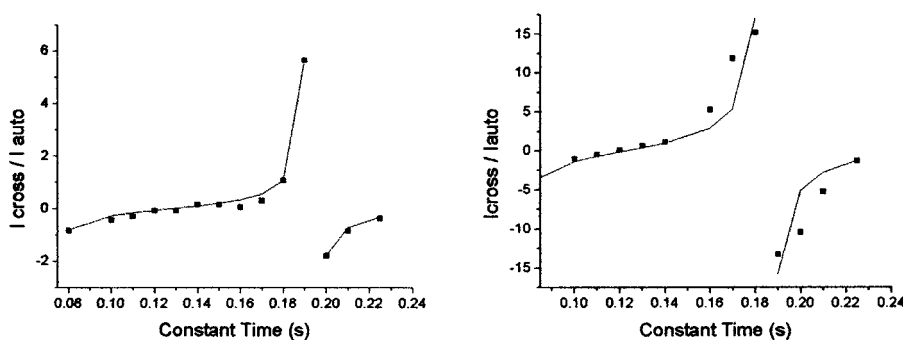


Figure 4. Fit of the  $I_{cross}/I_{auto}$  intensities for Gal H1-H2 signal of **1** with Method I to obtain  $^1J_{HH}$  ( $+^1D_{HH}$ ). (a) HSQC (sel C, sel H) CT-COSY. (b)  $^1H$ - $^1H$  CT-COSY. Plots on the left are for D<sub>2</sub>O sample and on the right for the CPCI 5% oriented sample.

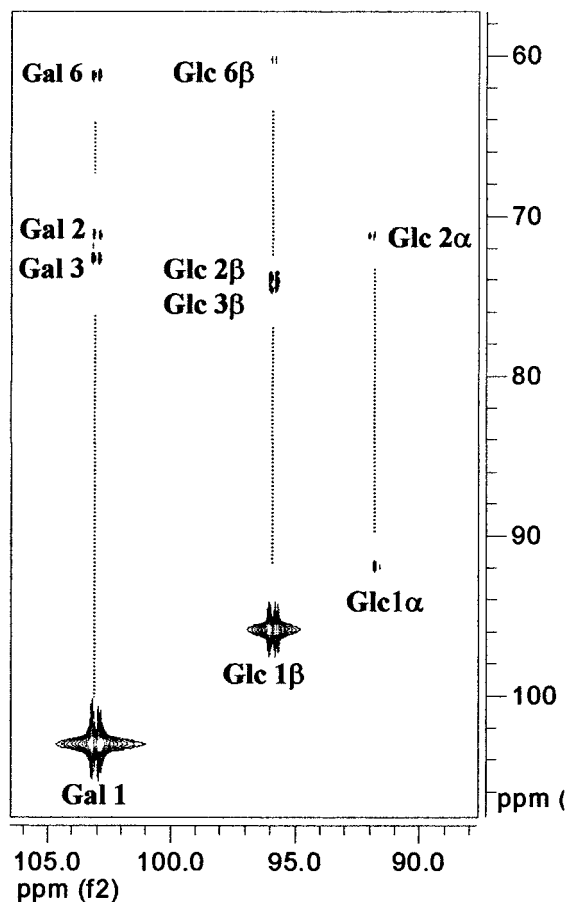


Figure 5. Anomeric region of the  $^{13}\text{C}$ - $^{13}\text{C}$  CT-COSY spectrum of **1** in  $\text{D}_2\text{O}$  ( $\Delta = 20$  ms). One-bond and long-range C-C correlations are visible.

Table 3. Long range  ${}^n\text{J}_{\text{CC}}$  couplings of **1** obtained at  $25^\circ\text{C}$  for the  $\text{D}_2\text{O}$  sample using Method II. Reference values were taken from Bose et al. (1998)

	Ref. (Hz)	${}^n\text{J}_{\text{CC}}$ (Hz)
Gal C1-C6	4.5	$4.46 \pm 0.1$
Gal C1-C3	4.6	$4.59 \pm 0.1$
Gal C3-C6	3.7	$3.67 \pm 0.1$
Glc $\beta$ C1-C6	4.2	$4.23 \pm 0.1$
Glc $\alpha$ C1-C6	3.3	$3.57 \pm 0.1$

### Measurement of ${}^n\text{J}_{\text{CC}}$

Long range C-C correlations are also observed in the 2D  $^{13}\text{C}$ - $^{13}\text{C}$  CT-COSY experiments (Figure 5). Indeed,  ${}^n\text{J}_{\text{CC}}$  are not totally unexpected, since for a pyranose in the chair conformation, several  ${}^3\text{J}_{\text{CC}}$  coupling pathways leave both  $^{13}\text{C}$  atoms with an antiperiplanar-type arrangement. This fact results in relatively large couplings, typically in the range 2.5–5 Hz, as described for simple monosaccharides (Bose et al., 1998). The measurement of  ${}^n\text{J}_{\text{CC}}$  can be useful to detect changes in the pyranose chair conformation, which may occur upon recognition by a biological receptor (Garcia-Herrero et al., 2002), and also may be used to determine the conformation around the glycosidic linkage (Bose et al., 1998).

Thus, additional 2D  $^{13}\text{C}$ - $^{13}\text{C}$  CT-COSY experiments were acquired with  $\Delta$  of 50–150 ms. In this range, the intensity dependence of the cross peaks became non linear, as required for quantitative analysis (Tian et al., 1999). Method I could not be used since at these large  $\Delta$  values, not only the active  ${}^n\text{J}_{\text{CC}}$  coupling, but also the one-bond passive coupling/s did modulate the  $I_{\text{cross}}/I_{\text{auto}}$  ratio. This effect that can be related to the differential relaxation of both peaks (Tian et al., 2001; Wu and Bax, 2001).  ${}^n\text{J}_{\text{CC}}$  were finally determined by using a modification (Method II) of the passive cross peak nulling method proposed by Wu and Bax (2001). The plot of the dependence of the calculated  $I'_{\text{cross}}$  intensities versus the constant time permitted to locate the different nulls. Then, the key null,  $\Delta_{\text{null}}$ , was determined allowing to estimate the correct  ${}^n\text{J}_{\text{CC}} = 1/2\Delta_{\text{null}}$ . The obtained results are given in Table 3 and an example of the analysis in Figure S5 in the supplementary material. The importance of the stereochemistry of the substituents attached to the  $^{13}\text{C}$  atoms is evident (i.e.,  ${}^3\text{J}_{\text{C1-C6}}$   $\alpha$  vs.  $\beta$ ) in the coupling values.

### Concluding remarks

For U- $^{13}\text{C}$ -saccharides, a 2D HSQC (sel C, sel H) CT-COSY experiment is proposed to measure many  $\text{D}_{\text{HH}}$ . The method is fast and fairly sensitive. It provides the magnitude and sign of all  $\text{D}_{\text{HH}}$  couplings mediated by both  ${}^n\text{J}_{\text{HH}} + {}^n\text{D}_{\text{HH}}$ .

A  $^{13}\text{C}$ - $^{13}\text{C}$  CT-COSY experiment is proposed for the accurate measurement of  ${}^1\text{J}_{\text{CC}} + {}^1\text{D}_{\text{CC}}$ . The method allows the determination of both the sign and magnitude of  ${}^1\text{D}_{\text{CC}}$ . The information provided by  ${}^1\text{D}_{\text{CC}}$



could be valuable for complexation studies of sugars with protein receptors. The high degree of orientation achieved for the saccharide in the bound state (Shimizu et al., 1999) may considerably increase the size of the RDC, also  $^1D_{CC}$ , making them sensitive to the conformational features in the bound state.

The  $^{13}C$ - $^{13}C$  CT-COSY experiment described herein permits the determination of  $^nJ_{CC}$ . These  $^nJ_{CC}$  are also structurally useful since they are sensitive to changes in the pyranose conformation and on the orientation around the  $\Phi/\Psi$  glycosidic torsion angles.

The sensitivity of these CT-COSY experiments largely depends on the  $\Delta$  constant time. During this period,  $T_2$  relaxation is taking place, decreasing the intensity of auto- and cross-peaks (Wu and Bax, 2001). The determination of small couplings requires large  $\Delta$  delays and the need of a proper fit of the intensities. This fact can compromise the sensitivity for polysaccharides or oligonucleotides with short  $T_2$  values. In addition, care should be taken when quantifying these couplings since non negligible differences in  $T_2$  relaxation of the two coupled nuclei involved may occur.

Alignment tensor calculations (Fischer et al., 1999; Azurmendi and Bush, 2002) for the application of these homonuclear RDC data (together with  $^1D_{CH}$ ) to obtain saccharide conformation in an NOE-independent manner are currently in progress and will be published elsewhere.

## Acknowledgements

The authors would like to thank Dr J.C. Cobas and Prof J. Sardina for their support with the MestRe-C v3.0 software (Cobas et al., 2003) used to analyze the data. The access to the NMR facility of the University of S. de Compostela is also acknowledged. We thank DGICYT for financial support (grant BQU2000-C1501).

## References

- Asensio, J.L., Cañada, F.J. and Jiménez-Barbero, J. (1995) *Eur. J. Biochem.*, **233**, 618–630.
- Azurmendi, H.F. and Bush, C.A. (2002) *J. Am. Chem. Soc.*, **124**, 2426–2427.
- Bax, A., Max, D. and Zax, D. (1992) *J. Am. Chem. Soc.*, **114**, 6923–6925.
- Bock K., Pedersen, C. and Pedersen, H. (1984), *Adv. Carbohydr. Chem. Biochem.*, **42**, 193–225.
- Bose, B., Zhao, S., Stenutz, R., Cloran, F., Bondo, P.B., Bondo, G., Hertz, B., Carmichael, I. and Serianni, A.S. (1998) *J. Am. Chem. Soc.*, **120**, 11158–11173.
- Cloran, F., Carmichael, I. and Serianni, A.S. (2000) *J. Am. Chem. Soc.*, **122**, 396–397.
- Cobas, J.C. and Sardina, F.J., submitted.
- Dwek, R.A. (1996) *Chem. Rev.*, **96**, 683–720.
- Fischer M.W.F., Losonczi, J.A., Weaver, J.L. and Prestegard, J.H. (1999) *Biochemistry*, **38**, 9013–9022.
- Freedberg, D.I., (2002) *J. Am. Chem. Soc.*, **124**, 2358–2362.
- Gabius, H.-J., Gabius, S. (Eds.) (1997) *Glycosciences: Status and Perspectives*, Chapman & Hall, London-Weinheim.
- Garcia-Herrero, A., Montero, E., Munoz, J.L., Espinosa, J.F., Vian, A., Garcia, J.L., Asensio, J.L., Canada, F.J. and Jimenez-Barbero, J. (2002) *J. Am. Chem. Soc.*, **124**, 4804–4810.
- Gomati, R., Appell, J., Bassereau, P., Maignan, J. and Porte, G. (1987) *J. Phys. Chem.*, **91**, 6203–6210.
- Hu, J. and Bax, A. (1996) *J. Am. Chem. Soc.*, **118**, 8170–8171.
- Hu, J. and Bax, A. (1997) *J. Am. Chem. Soc.*, **119**, 6360–6368.
- Jimenez-Barbero, J. and Peters, T. (Eds.) (2002) *NMR Spectroscopy of Glycoconjugates*, Wiley-VCH, Weinheim.
- Kupce, E., Boyd J. and Campbell, I.D. (1995) *J. Magn. Reson. B*, **106**, 300–303.
- Lycknert, K., Maliniak, A. and Widmalm, G. (2001) *J. Phys. Chem. A.*, **105**, 5119–5122.
- Martin-Pastor, M. and Bush, C.A. (2001) *J. Biomol. NMR*, **19**, 125–139.
- Neubauer, H., Meiler, J., Peti, W. and Griesinger, C. (2001) *Helv. Chim. Acta*, **84**, 243–258.
- Peti, W. and Griesinger, C. (2000) *J. Am. Chem. Soc.*, **122**, 3975–3976.
- Platzer, N., Davoust, D., Lhermitte, M., Bauvy, C., Meyer, D.M. and Derappe, C. (1989) *Carbohydr. Res.*, **191**, 191–207.
- Porte, G., Gomati, R., El Haitamy, O., Appell, J. and Maignan, J. (1986) *J. Phys. Chem.*, **90**, 5746–5751.
- Prestegard, J.H. (1998) *Nat. Struct. Biol.*, **5**, 517–522.
- Prosser, R.S., Losonczi, J.A. and Shiyonovskaya, I.V. (1998) *J. Am. Chem. Soc.*, **120**, 11010–11011.
- Rundlöf, T., Landersjö, C., Lycknert, K., Malinak, A. and Widmalm, G. (1998) *Magn. Reson. Chem.*, **36**, 773–776.
- Santoro, J. and King, G.C. (1992) *J. Magn. Reson.*, **97**, 202–207.
- Shimizu, H., Brown, J.M., Homans, S.W. and Field, R.A. (1998) *Tetrahedron*, **54**, 9489–9497.
- Shimizu, H., Donohue-Rolfe, A. and Homans, S.W. (1999) *J. Am. Chem. Soc.*, **121**, 5815–5816.
- Tian, F., Al-Hashimi H.M., Craighead, J.L. and Prestegard, J.H. (2001) *J. Am. Chem. Soc.*, **123**, 485–492.
- Tian, F., Bolon, P. and Prestegard, J. (1999) *J. Am. Chem. Soc.*, **121**, 7712–7713.
- Tian, F., Fowler, C.A., Zartler, E.R., Jenney Jr., F.A., Adams, M.W. and Prestegard, J.H. (2000) *J. Biomol. NMR*, **18**, 23–31.
- Tjandra, N. and Bax, A. (1997) *Science*, **278**, 1111–1114.
- Vincent, S.J.F. and Zwahlen, C. (2000) *J. Am. Chem. Soc.*, **122**, 8307–8308.
- Vuister, G.W. and Bax, A. (1992) *J. Magn. Reson.*, **98**, 428–435.
- Wu, Z. and Bax, A. (2001) *J. Magn. Reson.*, **151**, 242–252.